Cell

Targeted Deletion of AIF Decreases Mitochondrial Oxidative Phosphorylation and Protects from Obesity and Diabetes

J. Andrew Pospisilik,[1] Claude Knauf,[2] Nicholas Joza,[1] Paule Benit,[3] Michael Orthofer,[1] Patrice D. Cani,[2,4] Ingo Ebersberger,[5] Tomoki Nakashima,[1] Renu Sarao,[1] Gregory Neely,[1] Harald Esterbauer,[6] Andrey Kozlov,[7] C. Ronald Kahn,[8] Guido Kroemer,[9,10,11] Pierre Rustin,[3] Remy Burcelin,[2] and Josef M. Penninger[1,*]

[1]Institute of Molecular Biotechnology of the Austrian Academy of Science, Dr. Bohrgasse 3, 1030 Vienna, Austria

[2]Institut de Médecine Moléculaire de Rangueil (I2MR), INSERM U858/Equipe 2, IFR31, CHU Rangueil, BP 84225, 31432 Toulouse, France

[3]INSERM U676, Hôpital Robert Debré, 48, boulevard Serurier, 75019 Paris, France

[4]Université Catholique de Louvain, Faculty of Medicine, Unit PMNT, Av. E. Mounier, 73/69, 1200 Brussels, Belgium

[5]Center for Integrative Bioinformatics Vienna, Max F. Perutz Laboratories, Dr. Bohrgasse 3, 1030 Vienna, Austria

[6]Medical University Vienna Clinical Institute for Medical and Chemical Laboratory Diagnostic, Waehringer Guertel 18-20, Vienna, Austria

[7]Ludwig Boltzman Institute for Clinical and Experimental Traumatology, Lorenz Boehler Hospital, Donaueschingenstrasse 13, Vienna, Austria

[8]Joslin Diabetes Center, Department of Medicine, Harvard Medical School, Boston, MA 02215, USA

[9]INSERM, U848, 94805 Villejuif, France

[10]Institut Gustave Roussy, 94805 Villejuif, France

[11]Université Paris Sud-Paris 11, 39 rue Camille Desmoulins, 94805 Villejuif, France

*Correspondence: josef.penninger@imba.oeaw.ac.at

DOI 10.1016/j.cell.2007.08.047

SUMMARY

Type-2 diabetes results from the development of insulin resistance and a concomitant impairment of insulin secretion. Recent studies place altered mitochondrial oxidative phosphorylation (OxPhos) as an underlying genetic element of insulin resistance. However, the causative or compensatory nature of these OxPhos changes has yet to be proven. Here, we show that muscle- and liver-specific AIF ablation in mice initiates a pattern of OxPhos deficiency closely mimicking that of human insulin resistance, and contrary to current expectations, results in increased glucose tolerance, reduced fat mass, and increased insulin sensitivity. These results are maintained upon high-fat feeding and in both genetic mosaic and ubiquitous OxPhos-deficient mutants. Importantly, the effects of AIF on glucose metabolism are acutely inducible and reversible. These findings establish that tissue-specific as well as global OxPhos defects in mice can counteract the development of insulin resistance, diabetes, and obesity.

INTRODUCTION

Type-2 diabetes mellitus (T2DM), with over 6 million new cases reported per year, currently represents one of the world's chief economic and health care challenges. Associated in >50% of cases with obesity, diabetes results from an imbalance in insulin secretion and peripheral insulin responsiveness. While a correlative involvement for mitochondria in both of these processes has long been recognized, their exact etiological contribution toward diabetes and obesity remains unclear (Lowell and Shulman, 2005).

Mitochondrial dysfunction in humans is manifest as a variety of disorders with clinical outcomes largely dependent on the magnitude and tissue distribution of the impairment (Lane, 2006; Wallace, 1999). A number of recent studies have implicated impaired skeletal muscle OxPhos in the etiology of insulin resistance proposing a mechanism for the development of diabetes and obesity (Lowell and Shulman, 2005; Wisløff et al., 2005; Rabol et al., 2006). Microarray expression analyses have highlighted the coordinate downregulation of mitochondrial genes controlled by the regulators of mitochondrial biogenesis peroxisome proliferator-activated receptor γ coactivator 1α (PGC-1α) and nuclear respiratory factor 1 (NRF-1) in biopsies from insulin resistant subjects (Mootha et al., 2003; Patti et al., 2003). In addition, in vivo nuclear magnetic resonance studies have revealed a strong, inverse correlation between OxPhos function and insulin resistance in skeletal muscle in human patients (Petersen et al., 2003, 2004). By contrast, more recent work in human diabetic patients have both questioned the consistency of this correlation (Boushel et al., 2007) and extended correlations to include OxPhos changes in the liver and fat (Dahlman et al., 2006; Misu et al., 2007). Despite the profound

implications of these findings for diabetes and obesity, the causative or compensatory nature of primary mitochondrial OxPhos deficiencies remains an enigma.

We have previously shown that conditional deletion of the mitochondrial flavoprotein apoptosis inducing factor (AIF) in mice can initiate progressive OxPhos dysfunction (Joza et al., 2005; Susin et al., 1999). AIF was originally identified as a mitochondrial protein involved in cell death (Susin et al., 1999; Wissing et al., 2004). However, mutation analysis in numerous model organisms has now established that the primary physiological role of AIF is maintenance of a fully functional respiratory chain (Cheung et al., 2006; Joza et al., 2005; Vahsen et al., 2004). When deleted, this inner-mitochondrial membrane-associated protein leads to a progressive loss of respiratory chain function and activity (Joza et al., 2005; Vahsen et al., 2004). Here, we test and exploit the respiratory-chain-stabilizing properties of AIF to generate models of progressive OxPhos deficiency and ask the question whether primary defects in mitochondrial respiration cause insulin resistance, diabetes, and/or obesity. Our data provide novel insight into the role of AIF in respiratory chain function, implicate AIF as a prominent regulator of obesity and diabetes susceptibility, and provide genetic evidence that tissue-specific and global reductions in OxPhos can induce a state of insulin sensitivity and resistance to metabolic disease.

RESULTS

Generation of Muscle- and Liver-Specific *AIF* Knockout Mice

We previously reported that conditional deletion of AIF in mice initiates a progressive reduction in OxPhos (Joza et al., 2005; Vahsen et al., 2004). Since our initial report, the conditional AIF line has been crossed >8 times onto the C57BL/6 background, reducing the severity and slowing the kinetics of the mitochondrial deficiency triggered by *AIF* deletion. Crossing the conditional *AIF* mice ($Aif^{flox/flox}$) to those bearing a transgene for *cre*-recombinase under control of either the muscle creatine kinase promoter (Mck-*cre*) (Bruning et al., 1998) or the liver albumin promoter (Alb-*cre*) (Postic et al., 1999), we generated mice displaying muscle- or liver-specific OxPhos deficiencies ($AIF^{flox/y}$; Mck-*cre*/+ and $AIF^{flox/y}$; Alb-*cre*/+ respectively). Both MAIFKO (muscle-specific AIF knockout) and LAIFKO (liver-specific AIF knockout) pups were born healthy, viable, and at normal Mendelian ratios (Figures 1A and 1B). PCR and western blotting confirmed efficient deletion of the *AIF* allele specifically in striated muscle in MAIFKO mice and in the liver in LAIFKO animals (Figures 1C and 1D). Morphological, histological, and serum analyses to assess muscle and liver condition revealed no abnormalities at 8 weeks of age in either set of mice (Figures 1E and 1F; see Figures S1A–S1C in the Supplemental Data available with this article online).

Muscle- and Liver-Specific *AIF* Knockout Mice Exhibit Defective Mitochondrial Oxidative Phosphorylation

In order to test whether a primary OxPhos deficiency plays a causal role in insulin resistance, several criteria must be met. First, due to the importance of the respiratory chain to cellular function, the perturbations in OxPhos gene expression and function must be modest. Second, due to the distinct roles of respiratory chain subunits and the broad changes reported in human studies, the model should affect the OxPhos pathway in as generalized a fashion as possible (Mootha et al., 2003; Patti et al., 2003).

To assess the suitability of our model, we performed microarray analyses on hindlimb muscle (MAIFKO) and liver (LAIFKO) tissue obtained from 8-week-old AIF mutant mice and their littermate controls. Comparison with the previously published data sets linking OxPhos downregulation in muscle to insulin resistance in humans (Mootha et al., 2003; Patti et al., 2003) yielded >85% overlap in coordinate OxPhos expression pattern between each MAIFKO and LAIFKO data sets and those of human insulin resistant subjects (Figures 1G and 1H; Table S1). Included were downregulation of ~90% of the detectable NRF-1 regulated homologs and 100% of the detectable PGC-1α-responsive mouse homologs in MAIFKO mice (Table S1). Paralleling data from type 2 diabetic human subjects (Mootha et al., 2003; Patti et al., 2003), the majority of the observed reductions in OxPhos gene expression were modest in extent and highly coordinated (Figure 1I). Both the MAIFKO and LAIFKO microarray data sets were subject to gene-ontology-based analyses of 271 cellular pathways curated from the KEGG and BioCarta databases (Mootha et al., 2003; Tomfohr et al., 2005). Specific inactivation of *AIF* produced the statistically most robust modulation of the Oxidative Phosphorylation Pathway in each tissue data set (Figure 1J; Table S2). Inconsequential effects were observed on the expression of numerous cell death pathways. Further, ultrastructural and nucleic acid analyses revealed no obvious alteration in mitochondrial morphology or tissue mitochondrial DNA content (Figures S2A and S2B; Figure S3A). Thus, MAIFKO and LAIFKO mice display a tissue-specific decrease in OxPhos gene expression reminiscent of that observed in muscle of insulin resistant patients.

We next tested whether these changes in respiratory gene expression were manifest on protein and functional levels using western blot (Figure 2A) and spectrophotometry/polarography of isolated mitochondria (Figure 2B). Corroborating our previous findings (Joza et al., 2005; Vahsen et al., 2004), complexes I and IV of the respiratory chain were functionally affected by loss of AIF expression in muscle, while liver-specific deletion of AIF was manifest primarily as a combined complex I and complex V deficiency (Figure 2B). Consistent with data from humans (Petersen et al., 2003), expression of muscle respiratory chain components decreased with age in both control and mutant MAIFKO animals (Figures S3B and S3C).

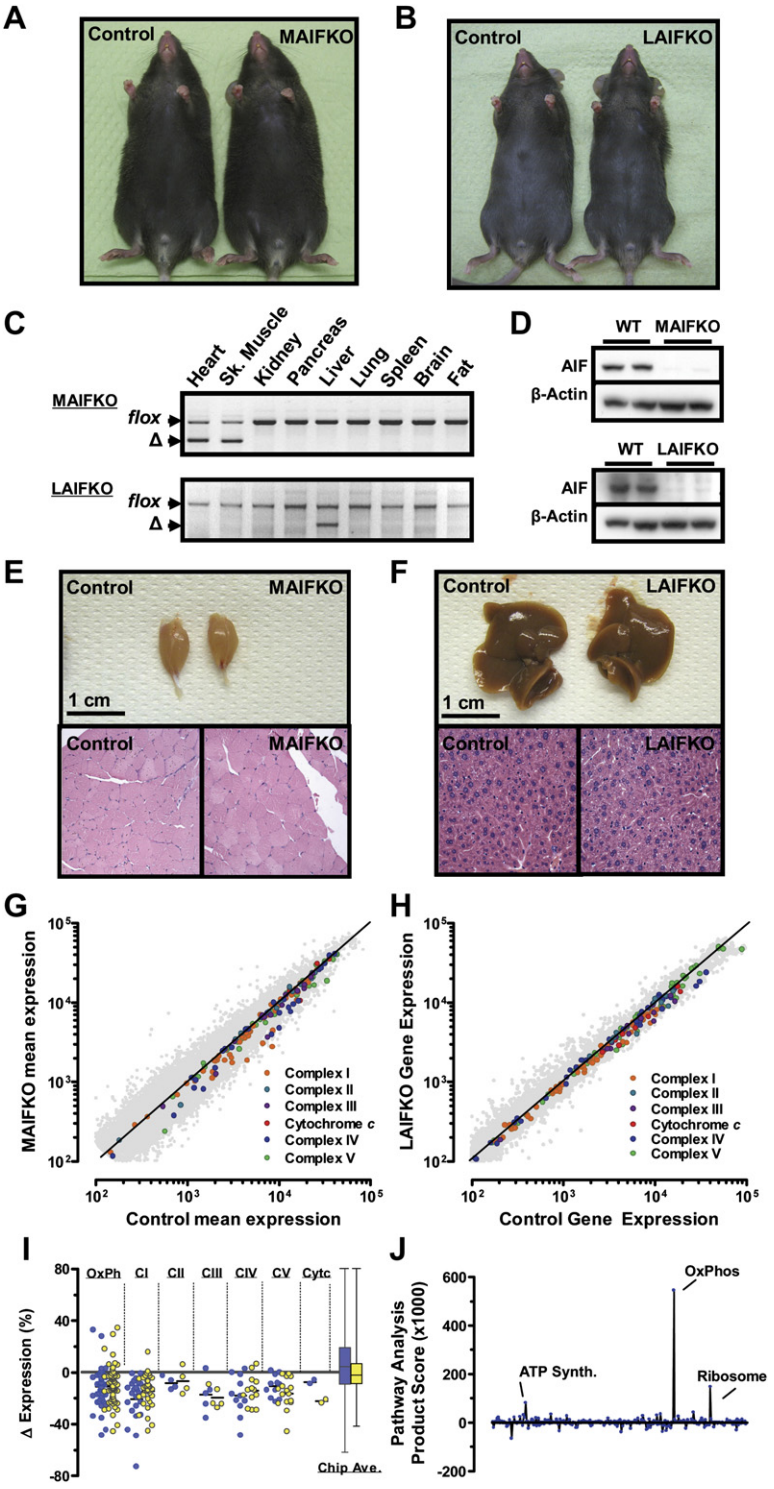

Figure 1. Muscle- and Liver-Specific *AIF* Knockout Mice Display Normal Tissue Morphology and Exhibit a Deficiency in OxPhos Gene Expression

(A) Muscle-specific (MAIFKO) and (B) liver-specific AIF knockout mice (LAIFKO) mice develop and grow normally until at least 2 months of age. (C) Deletion of *loxP* flanked exon 7 of the *Aif*-allele (Aif^{flox}) by Mck- or Alb-driven transgenic *cre* recombinase result in muscle- and liver-specific *AIF* deletion (Aif^{-}), confirmed here by PCR and (D) Western blot. Target tissue isolations and histological analysis by H&E staining showed normal tissue and cellular morphology in both MAIFKO (E) and LAIFKO (F) mice. (G and H) Microarray analyses of targeted tissues from 8-week-old MAIFKO and LAIFKO mice revealed coordinate downregulation of genes of oxidative metabolism. These reductions overlapped in >85% of cases with human orthologs reported previously to be downregulated in humans with insulin resistance (OxPhos) (Mootha et al., 2003; Patti et al., 2003) and (I) with individual complexes of the electron transport chain. (J) Gene-ontology-based analysis confirmed that of 272 curated pathways (KEGG/BioCarta), OxPhos and ATP synthesis are two of the three most significantly modulated pathways in both muscle and liver after AIF deletion. The product score is a measure of deviation of pathway expression combined for both the muscle and liver data sets.

Examination of functional markers of OxPhos confirmed the defects with an increase in NADH/NAD^+ ratios and decreased ATP and cAMP levels in both MAIFKO and LAIFKO knockout tissues (Figures 2C and 2D; Figure S3D). Plasma lactate, a marker of anaerobic metabolism, was found to be modestly elevated in MAIFKO and LAIFKO mice, corroborating the finding of reduced OxPhos function in vivo (Tables S3 and S4).

The third criterion necessary to model the OxPhos dependency of insulin resistance is dissociability of OxPhos modulation from ROS generation. ROS are byproducts of electron flux through OxPhos and are metabolites known

to cause insulin resistance (Balaban et al., 2005; Houstis et al., 2006; St-Pierre et al., 2006). Produced primarily at complex I (directed internally) and complex III (directed externally), the generation of ROS is dependent on the rate of flux through the respiratory chain as well as the degree of distal restrictions to electron flow (Adam-Vizi and Chinopoulos, 2006). Direct measurement of mitochondrial ROS production using EPR-spectroscopy revealed no significant changes in either internally or externally generated ROS in preparations from MAIFKO or LAIFKO mice (Figures 2E and 2F). These findings were corroborated by a lack of detectable change in the ROS markers catalase, protein carbonylation, and lipid peroxidation (Figures S3E–S3G). Western blot analysis of the ROS- and inflammation-responsive signals JNK, IκB, and ERK5 (Nakano et al., 2006) showed no alteration in either muscle- or liver-specific AIF knockout mice at 8 weeks of age (data not shown). No histological signs of inflammation, nor increased serum levels of the inflammatory cytokines IL-6 and TNF-α were observed. These findings suggest that loss of AIF does not cause either ROS accumulation or the induction of inflammation. Thus, tissue-specific AIF deletion satisfies all three criteria of moderate, generalized, and ROS dissociable OxPhos reduction providing a model to test whether primary defects in mitochondrial respiration cause insulin resistance and obesity.

Enhanced Respiratory Control and Altered Substrate Access in AIF-Deficient Mitochondria

Changes in OxPhos should be reflected by modifications in ROS generation unless (1) the balance between respiratory coupling and uncoupling is altered, or (2) the access of electrons to sites of ROS generation is modified by alternate electron entry into the respiratory chain. Isolated MAIFKO and LAIFKO mitochondria were examined for their inherent coupling capacity and substrate selectivity. O_2-consumption in AIF-deficient mitochondria was more efficiently reduced by addition of the ATPase inhibitor oligomycin than in controls, indicating electron transport is more tightly coupled to ATP-synthesis in the absence of AIF (Figures 2G and 2H). Further, reduced O_2-consumption rates measured subsequent to addition of the mitochondrial uncoupler mC1-CCP (carbamoyl cyanide m-chlorophenylhydrazone) highlighted the decreased activity of the OxPhos chain in AIF-deleted mitochondria (Figure 2G). Interestingly, parallel measurements of substrate selectivity revealed a preference for non-complex-I electron donors such as succinate (complex II) and glycerol-3-phosphate (G3P) in AIF deficient mitochondria (Figure 2I; Figure S3H). These findings were corroborated by measured increases in succinate-cytochrome c reductase (SCCR) and glycerol-3-phosphate-cytochrome c reductase activities (GCCR) in both muscle and liver mitochondria of *AIF* knockout mice (Figure S3I). Thus, AIF ablation reduces complex-I derived electron transfer and mitigates ROS generation through increased respiratory chain coupling.

Targeted Deletion of AIF in Muscle Results in Improved Glucose Tolerance and Insulin Sensitivity

Since at 8 weeks of age both models demonstrated consistent OxPhos deficiency with no indication of elevated ROS levels, this time point was chosen for all subsequent metabolic analyses. Intriguingly, initial metabolic analyses revealed an improvement in oral glucose tolerance in MAIFKO mice (Figure 3A, top). Reduced fasting and challenged blood glucose levels observed during oral glucose tolerance testing (OGTT) occurred concomitantly with reduced insulin secretion suggestive of an increase in insulin sensitivity (Figure 3A, bottom). In line with these findings, blood glucose and insulin levels were reduced during normal feeding cycles (Table S3). Moreover, intraperitoneal insulin challenge resulted in enhanced blood glucose lowering in MAIFKO mice (Figure 3B). To validate these indications of increased insulin sensitivity, a euglycemic-hyperinsulinemic clamp was performed. Upon infusion of insulin, MAIFKO mice displayed an immediate and robust increase in glucose demand (Figure 3C). This increase in insulin sensitivity was characterized by elevated steady-state (measured between 150 and 180 min) glucose turnover (Figure 3D) as well as augmented glycogen synthesis rates (Figures 3E and 3F) and a tendency toward increased hepatic glucose production and whole body glycolysis (Figures S4A and S4B). Thus, ablation of AIF in muscle elicits an insulin-sensitive state.

Introduction of radiolabeled 2-deoxyglucose into the clamp protocol revealed increased glucose flux into all skeletal muscles tested but not the heart, skin, liver, or brown adipose tissue (BAT) (Figure 3G). To link the increased glucose uptake to critical nodes in the insulin signaling cascade (Taniguchi et al., 2006), western blot analysis on muscle extracts from insulin-clamped animals was performed. Phosphorylation of Akt, ERK1/2, and GSK3β were increased in MAIFKO mice following insulin infusion (Figure 3H, right panels; Figure S4C). Interestingly, despite reduced fasting insulin levels (Table S3), ERK1/2 and GSK3β were also increased under fasting conditions (Figure 3H, left panels; Figure S4C), indicating increased basal activation of insulin signaling. Also, expression of the two primary muscle glucose transporters GLUT1 and GLUT4 was upregulated in MAIFKO mice (Figure 3I). Examination of the key metabolic regulator AMPK revealed increased activation of this AMP sensor with no apparent change in AMPK protein expression (Figure 3J). Thus, AIF-deletion in muscle causes improved insulin sensitivity characterized by increased muscle glucose uptake, enhanced insulin signaling, and general upregulation of glucose uptake machinery.

MAIFKO Mice Are Resistant to Diet-Induced Obesity and Diabetes

In humans and wild-type mice, high fat diet induces obesity, insulin resistance, and diabetes (Lazar, 2005). MAIFKO and littermate control mice were challenged with a high-fat diet from weaning and analyzed at 8 weeks of age. Control mice fed a high-fat diet developed obesity

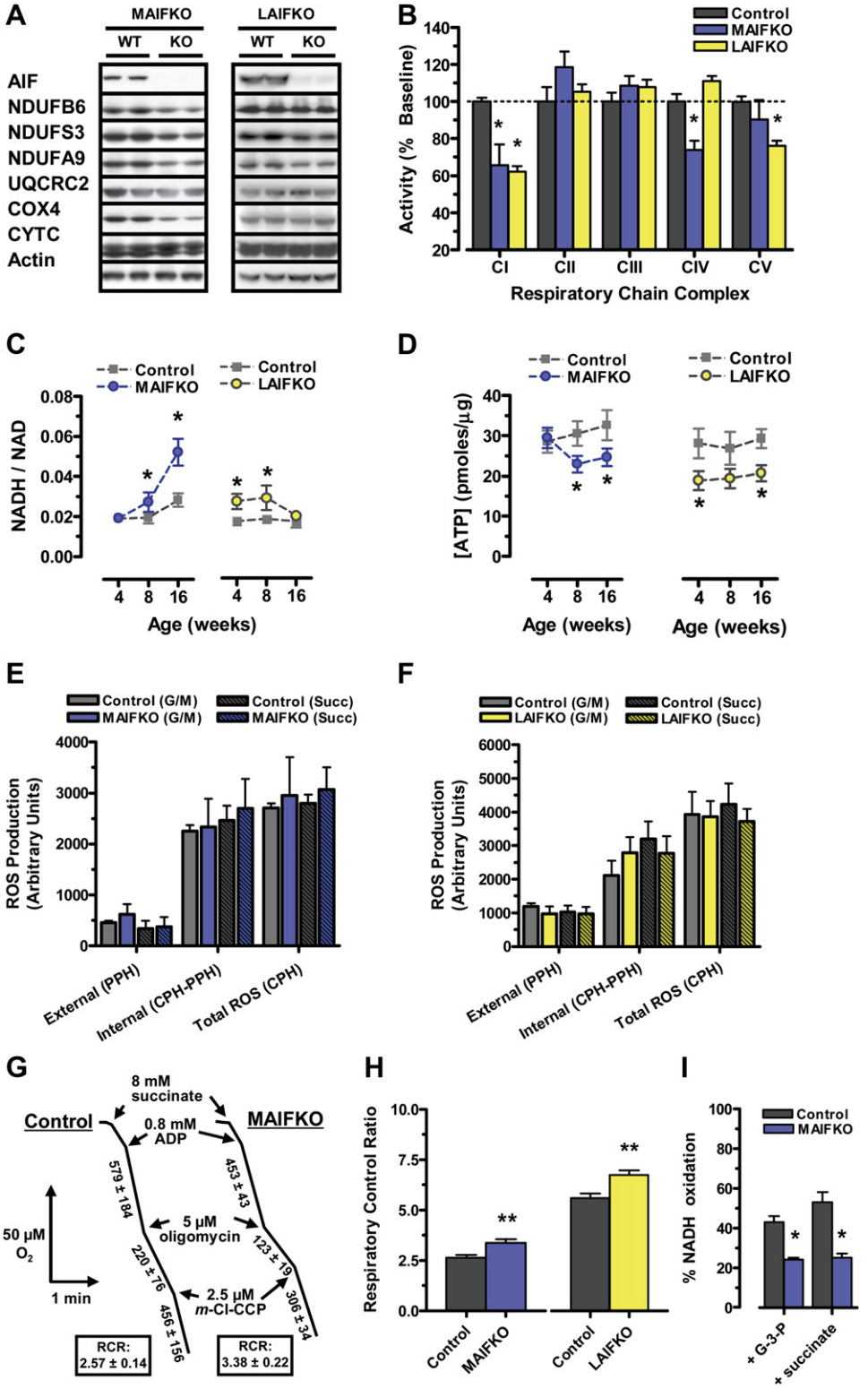

Figure 2. Tissue-Specific Deletion of AIF in Muscle and Liver Results in OxPhos Defects

(A and B) Reductions in OxPhos gene expression were confirmed on the (A) protein and (B) functional levels in both MAIFKO and LAIFKO target tissues (NDUFx, complex I subunits; UQCRC2, complex III subunit C2; COX4, complex IV subunit 4; CYT C, cytochrome c). AIF expression is shown as a control for genotypes, and actin is shown as a loading control. OxPhos activities of individual respiratory complexes were assessed on isolated mitochondria by spectrometry and polarography.

as determined by progressive weight gain (Figure 4A), increased lipid accumulation in adipocytes (Figure 4B), and enhanced fat pad mass (Figure 4C). However, despite a significant elevation in food intake (Figure 4D), MAIFKO mice failed to gain additional weight or to accumulate lipids relative to normal chow fed mutants (Figures 4A–4C). Consistent with the reduction in adipose mass, plasma leptin levels in MAIFKO mice were markedly decreased (Figure 4E). We failed to observe alterations in lipid handling in MAIFKO mice whether by plasma cholesterol, triglyceride, or free fatty acid (FFA) determination (Table S3) or by measurement of free fatty acid release in response to fasting (Figure S4D). Moreover, indirect calorimetry and activity measurements did not reveal overt alterations in metabolic rate, respiratory quotient (nutrient partitioning), activity, or energy expenditure in MAIFKO animals (Figure S5A–S5C).

In addition to the development of obesity, control mice fed a high-fat diet develop diabetes defined by fasting hyperglycemia and hyperinsulinemia as well as increased glucose and insulin levels after an oral glucose challenge (Figures 4F–4H). MAIFKO mice resisted the diabetogenic effects of the high fat diet (Figures 4F–4H). As evidenced by a moderate increase in glucose-challenged insulin levels in MAIFKO mice on high-fat chow, some metabolic deterioration was still observed in these tissue-specific mutants (Figure 4G). Importantly, whereas littermate controls exhibited insulin resistance, MAIFKO mice were still sensitive to the glucose-lowering effects of insulin (Figure 4I). Thus, muscle-specific ablation of AIF prevents diet-induced obesity and diabetes.

Improved Metabolic Phenotypes in *AIF* Mosaic Mice

We have previously reported that muscle specific *AIF* knockout mice eventually succumb to muscle wasting and dilated cardiomyopathy (Joza et al., 2005). To eliminate the possibility of experimental bias from these alternate pathologies, we exploited localization of the *AIF* gene on the X chromosome (Susin et al., 1999) to generate a set of mice with a mosaic muscle-specific AIF knockout pattern based upon random epigenetic X-inactivation ($AIF^{flox/+}$; Mck-cre/+). These mice exhibit mosaic expression of wild-type or deleted *AIF* alleles in muscle and, beyond 8 months of age, continue to grow normally and show no evidence of muscle wasting, cachexia, or cardiomyopathy (Figure 5A; data not shown). Importantly, these mosaic mice recapitulate the lean phenotype of muscle-specific *AIF* null animals (Figures 5B and 5C). Moreover, determination of glucose handling showed that AIF mosaic mice exhibit improved glucose tolerance and reduced insulin levels (Figures 5D–5F). Similar to MAIFKO mice, metabolic rate, respiratory quotient, activity, and energy expenditure were comparable between mosaic MAIFKO and control littermates (Figures S5D–S5F). These results dissociate possible influences from secondary pathologies over the long term and confirm that inactivation of AIF in muscle cells can protect from weight gain and insulin resistance.

Liver-Specific AIF Knockout Mice Are Glucose Tolerant and Resist Obesity and Diabetes

In addition, the liver has been implicated in the development of insulin resistance and demonstrated OxPhos changes in humans (Misu et al., 2007). Examination of glucose control by OGTT in liver-specific *AIF* knockout (LAIFKO) mice, similar to MAIFKO animals, revealed marked improvements in glucose tolerance characterized by decreases in both peak blood glucose and insulin levels relative to control animals (Figure 6A). Also, LAIFKO mice displayed a hyper-responsiveness to i.p. insulin injection (Figure 6B). In euglycemic-hyperinsulinemic clamp studies, LAIFKO animals required increased glucose infusions (GIR) (Figures 6C and 6D) and exhibited significantly increased glucose turnover (Figure 6D). Hepatic glucose production remained unchanged (Figure 6D). Consistent with increased anaerobic metabolism, we observed increased glycolysis (Figure 6D). Considering the age-dependence of diabetes and obesity as well as the progressive nature of OxPhos deficiencies (Lowell and Shulman, 2005; Wallace, 1999), we asked whether the glucose tolerant LAIFKO phenotype would change with time. Glucose tolerance tests performed at 8, 16, and 52 weeks of age showed significant improvements in glucose tolerance of LAIFKO mice at all ages (Figure 6E), indicating that increased insulin sensitivity was maintained with aging. Intriguingly, despite a reduction in plasma insulin levels after fasting (Table S4), the critical insulin signaling components ERK1/2 and GSK3β again showed heightened activation in the knockout animals (Figure 6F). In addition, expression of the glucose transporter GLUT1 levels as well as activation of AMPK and expression of nutrient sensor SIRT1 were increased in vivo (Figure 6F). Thus, loss of AIF expression in hepatocytes results in increased insulin sensitivity.

We next examined whether liver-specific loss of AIF would render mice resistant to high-fat feeding. Whereas

(C and D) Decreases in relative NAD^+ and ATP levels served as a functional readout of the cellular consequences of reduced OxPhos in both MAIFKO and LAIFKO mice.

(E and F) Direct measurement of ROS generation in isolated target tissue mitochondria by EPR-spectroscopy showed no elevation in ROS levels in either MAIFKO or LAIFKO mice. Measurements of ROS production both inside and outside the mitochondria were made using the spin trap CPH (total ROS). ROS produced externally were evaluated using the membrane impermeable spin trap PPH (external). Internally generated ROS production was determined by subtraction (internal).

(G and H) Mitochondria isolated from *AIF*-deficient muscle and liver displayed increased respiratory coupling relative to controls when assessed using polarography.

(I) Spectrophotometric analysis revealed altered substrate preference through monitoring of substrate competition between NADH oxidation and oxidation of succinate or glycerol-3-phosphate. All measures were made using 8-week-old mice. $AIF^{flox/y}$ mice served as controls. All data are mean ± SEM. n = 4–9 per group. *$p < 0.05$ versus control.

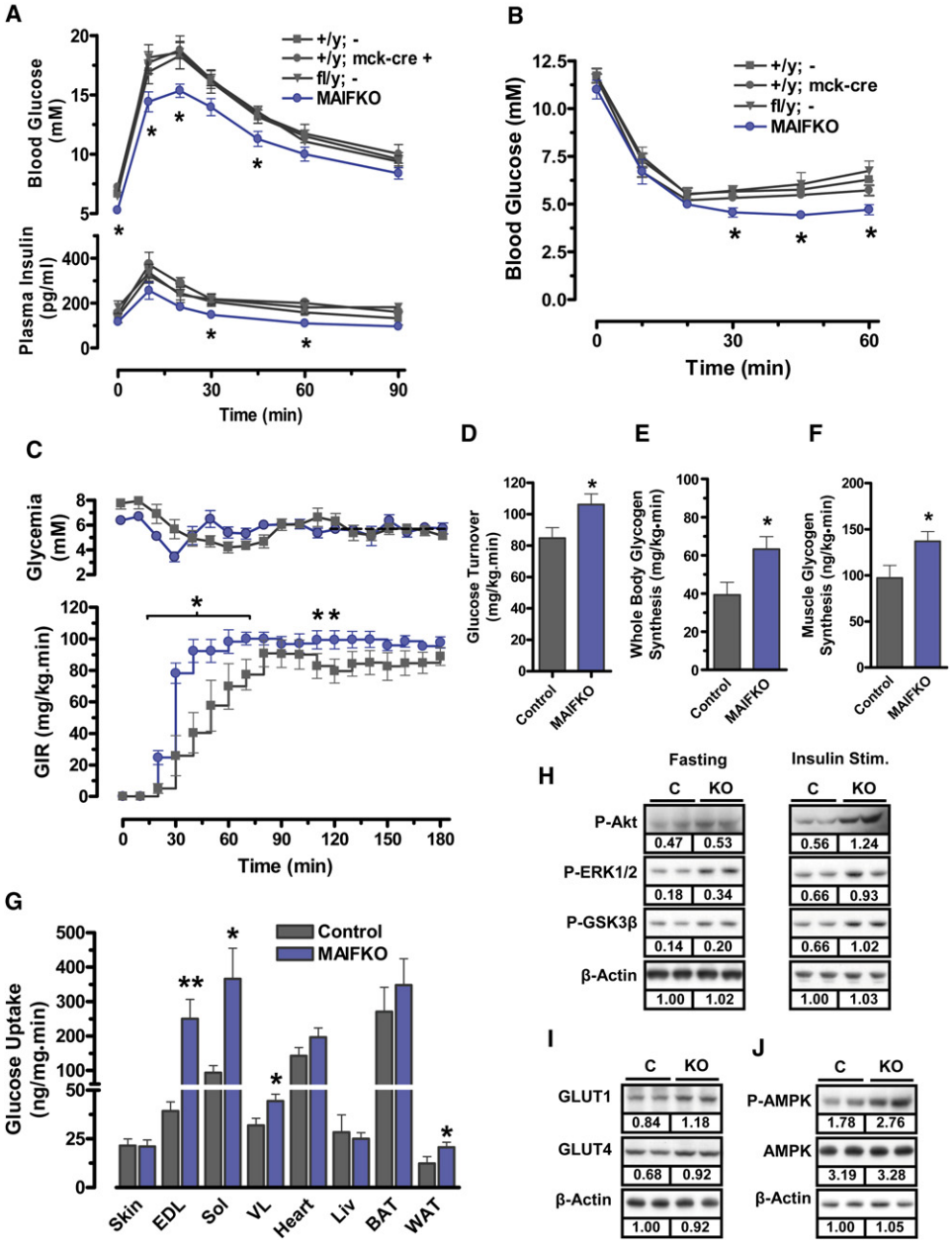

Figure 3. Targeted-Ablation of AIF in Muscle Causes Improved Glucose Tolerance and Insulin Sensitivity

(A) Relative to all three control littermate genotypes (wild-type, Mck-*cre* hemizygote, and *AIF*$^{flox/y}$), MAIFKO mice exhibit reduced blood glucose levels and reduced plasma insulin excursions in response to a 1 g/kg oral glucose load.

(B) Bolus injection of insulin intraperitoneally elicits a more profound glucose reduction in MAIFKO mice relative to littermate controls.

(C) Plasma glucose and glucose infusion rates, measured during a euglycemic hyperinsulinemic clamp, reveal increased insulin-induced glucose demand in MAIFKO mice.

(D–F) The measured increase in insulin sensitivity was characterized by increased whole-body glucose turnover as well as increased whole body and muscle specific- glycogen synthesis.

(G) Including labeled 2-deoxyglucose into the clamp protocol revealed enhanced glucose uptake in skeletal muscle depots of mutant mice (EDL, extensor digitorus longus; Sol, soleus; VL, vastus lateralis; BAT, brown adipose tissue; WAT, white adipose tissue). Data in (A)–(G) are mean ± SEM. n = 8–10 per group. *p < 0.05 versus littermate controls.

(H) Consistent with the observed increases in insulin sensitivity, enhanced phosphorylation of ERK1/2, Akt, and GSK3β were observed in both fasted and insulin stimulated (clamped for 3 hr) muscle tissue by western blotting.

(I) Protein expression of the glucose transporters 1 and 4 (GLUT1 and GLUT4) were increased in MAIFKO muscle.

(J) Elevated AMPK phosphorylation in muscle of MAIFKO mice. In (H)–(J), data pooled data (2 mice per lane) from four individual control and four individual MAIFKO mice are shown. β-Actin is shown as a loading control. All animals were 8 weeks of age. Controls are *AIF*$^{flox/y}$.

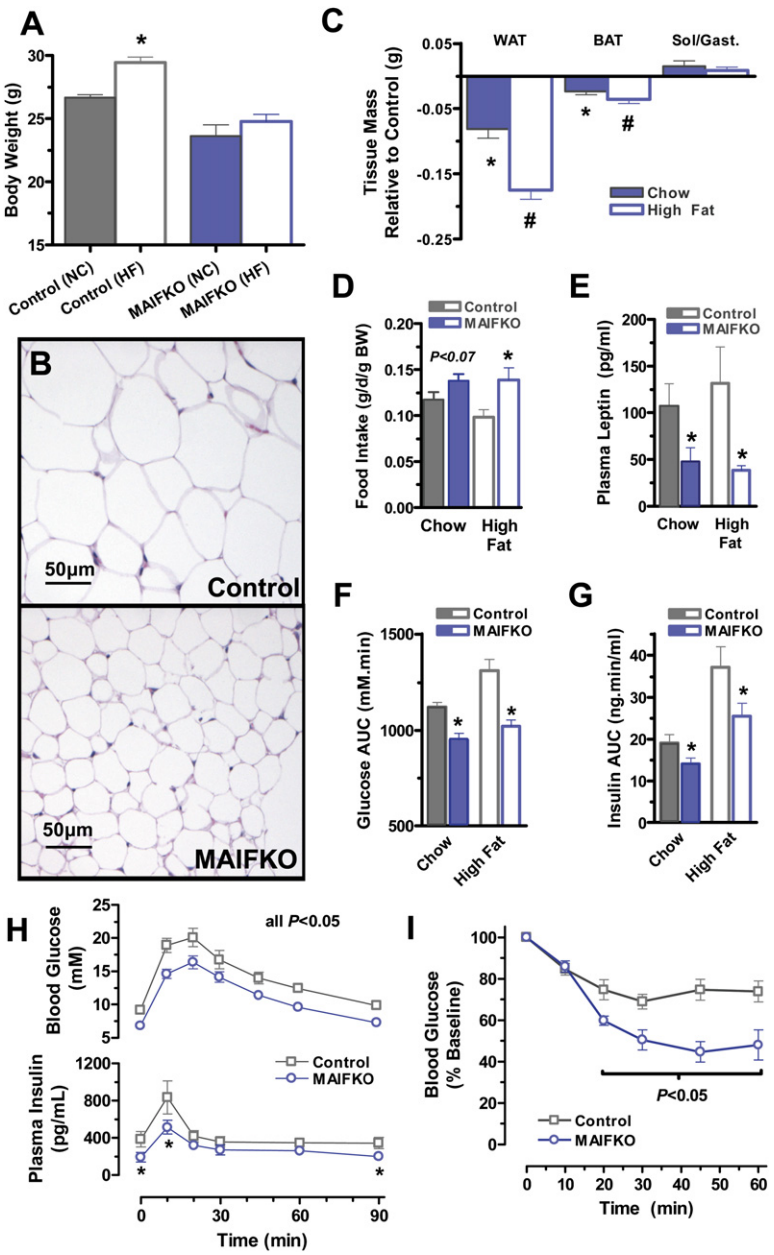

Figure 4. MAIFKO Mice Are Resistant to Diet-Induced Obesity and Diabetes

(A) High-fat feeding (HF; open symbols) promotes adiposity in control, but not MAIFKO, animals. Closed symbols are from mice fed with normal chow (NC). Mice were fed a high-fat diet from 3 to 8 weeks of age at which time all presented metabolic analyses were performed.

(B–C) Reduced development of adiposity was seen at the cellular level by H&E staining as well as by determination of white (perigonadal; WAT) and brown adipose tissue (BAT) masses after both normal chow and high-fat diet. Data in (C) are shown as knockout tissue mass relative to control tissue mass.

(D) Reduced adiposity in MAIFKO mice occurred despite increased food intake. Food intake was determined over 48 hr in metabolic cages.

(E) Consistent with reduced fat mass, circulating leptin levels were reduced in MAIFKO animals relative to control littermates. Food intake was determined over 48 hr in metabolic cages.

(F–H) Oral glucose tolerance testing revealed maintenance of the glucose tolerant and insulin sensitive state after high-fat feeding. AUC, area under the curve.

(I) An insulin tolerance test showed a clear separation in the ability of MAIFKO mice to clear glucose after a defined insulin load (1.5 U/kg i.p.). Data are mean ± SEM. n = 6–10 animals per group. *p < 0.05 versus control. Controls are $AIF^{flox/y}$. NC, normal chow diet; HF, high-fat diet; WAT, white adipose tissue; BAT, brown adipose tissue.

control mice gained 17% body weight over this time frame of high-fat feeding, LAIFKO mice gained only 2% relative to normal chow fed LAIFKO mice (Figure 7A). Measurement of epididymal fat pad weights confirmed marked adipose deposition in control animals with no discernable impact on the knockout animals (Figures 7B–7D). The described resistance to adipose deposition occurred despite an increase in food intake. Food intake in normal chow fed LAIFKO mutants was also moderately elevated (Figure 7E). The metabolic rate, respiratory quotient, activity, and energy expenditure were comparable between mosaic MAIFKO and control littermates (Figures S5G–S5J). No obvious differences in differentiation and functional markers of brown and white adipose tissue were detected in either MAIFKO or LAIFKO mice at the transcriptional level (Figures S6A and S6B). In addition, an examination of intracellular lipids in muscle and liver tissues of AIF mutant mice revealed no overt changes in triglyceride (Figures S7A and S7B) or long chain fatty acyl CoA's (Figures S7C and S7D). These data suggest that the lean phenotype of muscle or liver specific AIF mutant mice does not result from overt changes in adipose tissue reprogramming.

When tested for glucose tolerance after chronic high-fat feeding, control mice exhibited increased blood glucose and insulin levels. By contrast, glucose and insulin values in high fat fed LAIFKO mice remained comparable to those of chow fed controls (Figure 7F). While some metabolic

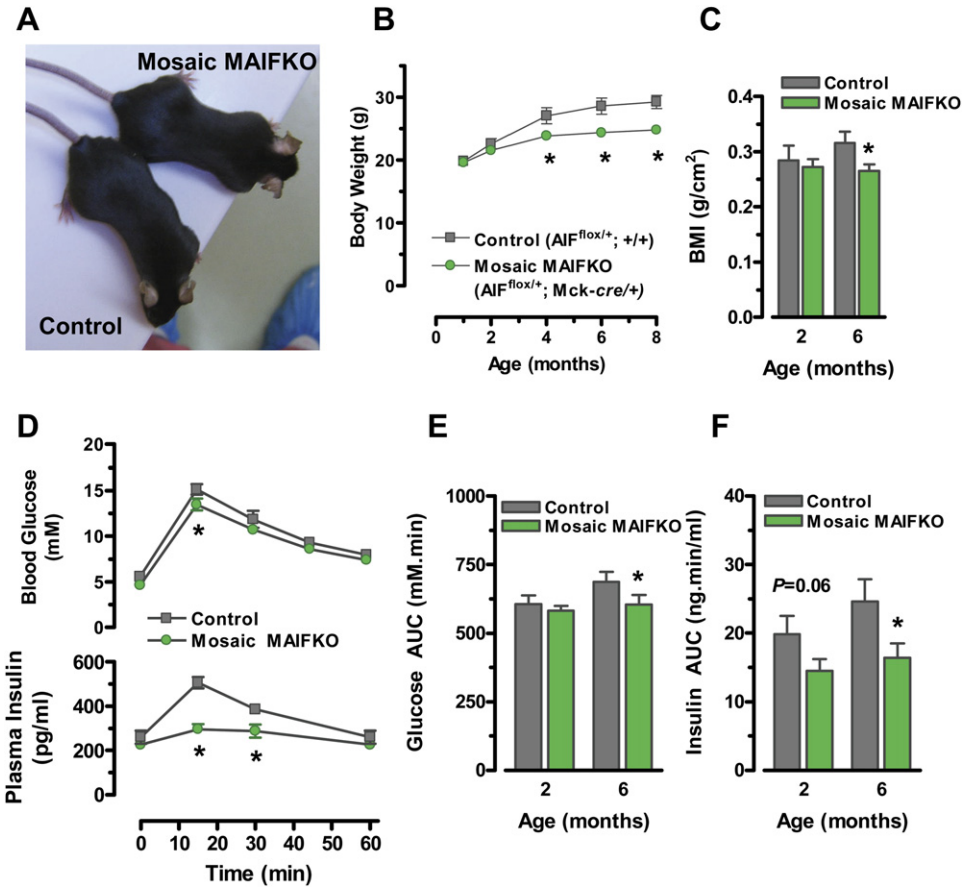

Figure 5. Mosaic Patterning of the AIF Deletion in Muscle Improves Glucose Tolerance

(A) To circumvent the premature mortality exhibited by MAIFKO mice, mice were generated exhibiting mosaic patterning of the *AIF* deletion in muscle. Since *AIF* is located on the X chromosome, *cre*-bearing $AIF^{flox/+}$ female heterozygotes will alternately exhibit either wild-type or deleted AIF as a consequence of random X-inactivation. These mice are born and grow normally and exhibit no obvious pathologies up to and beyond 8 months of age.

(B and C) Measurement of body weight and body mass index (BMI) in these mice confirmed the lean phenotype. BMI (body mass index) = [weight (g)/length^2 (cm^2)].

(D) Oral glucose tolerance testing (1 g/kg) in 6-month-old mosaic mice reveals a moderate improvement in glucose tolerance with a considerable reduction in peak insulin levels.

(E and F) Reductions in blood glucose and plasma insulin levels appeared progressive, with a trend already obvious at 2 months of age (i.e., prior to any changes in body weight). Data are mean ± SEM. n = 6 animals per group. *$p < 0.05$ versus control.

deterioration was observable, e.g., increased insulin relative to chow-fed LAIFKO animals (Figure 7F), insulin tolerance testing further confirmed that LAIFKO mice maintain an insulin sensitive phenotype even after high-fat feeding (Figure 7G). As with the MAIFKO mice, we failed to observe altered lipid handling in the LAIFKO mouse (Figure S7; Table S4). Thus, deletion of AIF in the liver, similar to muscle-specific deletion, induces a lean and insulin sensitive metabolic state, conferring resistance to the adipogenic and diabetogenic effects of hypercaloric feeding.

Improved Insulin Sensitivity in Mice with a Ubiquitous OxPhos Defect

To examine the possibility that a multisystem OxPhos defect, rather than a muscle- or liver-specific deficiency, may account for the correlative development of insulin resistance in human subjects (Dahlman et al., 2006), we analyzed a global model of OxPhos deficiency, the *harlequin* mouse (Hq). While ubiquitous disruption of the *Aif*-allele is embryonic lethal (Joza et al., 2005), AIF-hypomorph Hq mice manifest a proviral intron insertion in the *AIF* gene as an ubiquitous 80% reduction in AIF protein expression and associated AIF-dependent OxPhos defects (Vahsen et al., 2004; van Empel et al., 2005). Similar to both muscle- and liver-specific *AIF* mutants, AIF-hypomorph Hq mice were resistant to the progressive weight gain and lipid accumulation associated with high-fat feeding (Figures 8A and 8B). Food intake was increased in the Hq mice (Figure 8C). Moreover, relative to littermate controls, Hq mice displayed improved glucose tolerance associated with reduced fasting and glucose-induced insulin

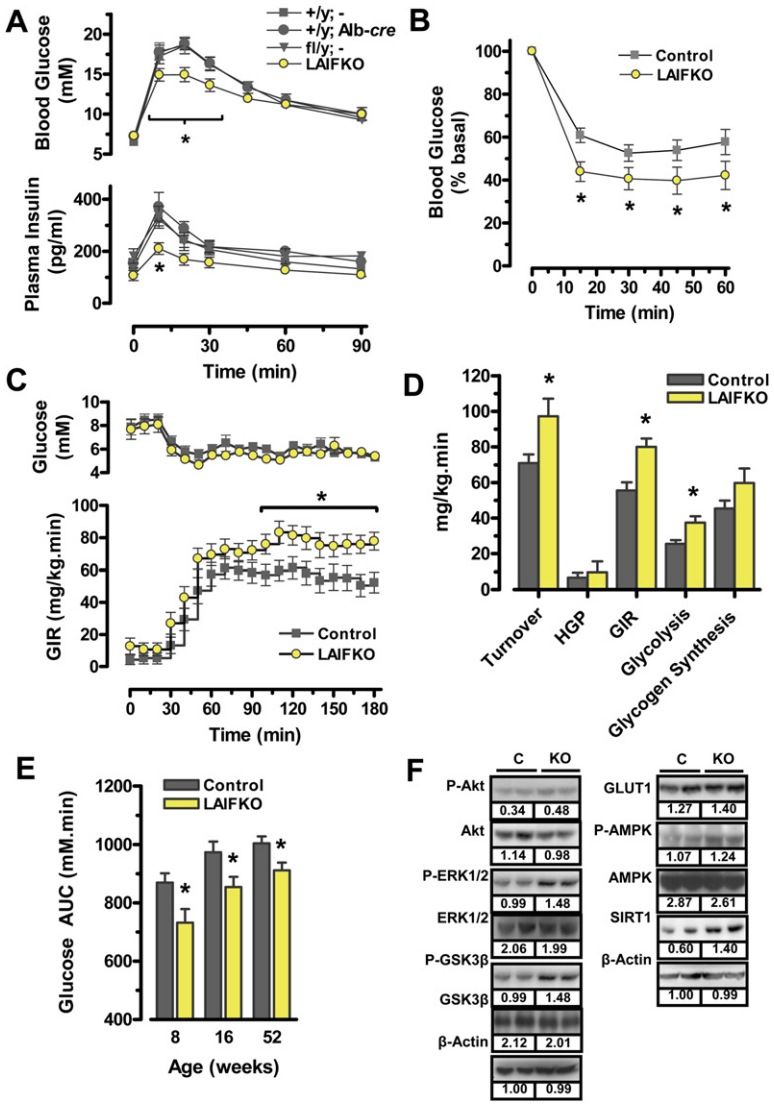

Figure 6. Improved Glucose Disposal and Insulin Sensitivity after *AIF* Deletion in a Second Insulin-Responsive Tissue, the Liver

(A) Relative to the three control littermate genotypes (wild-type, Alb-*cre* hemizygote, and $AIF^{flox/y}$), LAIFKO mice exhibited reductions in plasma glucose and insulin levels after a 1 g/kg oral glucose challenge.

(B) LAIFKO mice exhibit an exacerbated hypoglycaemic response to intraperitoneal insulin (0.75 U/kg) relative to littermate controls.

(C) In response to a 4 mU/min/kg chronic insulin infusion, LAIFKO mice required a significantly increased glucose infusion (GIR) relative to Control mice in order to maintain euglycemia.

(D) The measured increase in insulin sensitivity was characterized by increased whole-body glucose turnover, increased GIR, increased glycolysis, and no change in hepatic glucose production (HGP). There was a tendency, albeit not significant, toward increased glycogen synthesis.

(E) Evidence of increased insulin sensitivity provided by oral glucose tolerance tests (OGTTs) that was maintained at least up to 1 year of age in LAIFKO mice. Data in (A)–(E) are mean ± SEM. n = 6–12 per group. *p < 0.05 versus littermate controls.

(F) Increased phosphorylation of the key insulin signaling intermediates ERK1/2, Akt, and GSK3β were observed in fasted LAIFKO livers. Also observed by western blotting were increases in expression of GLUT1 and SIRT1, as well as phosphorylation of the AMP-responsive AMPK. β-Actin is shown as a loading control. C, Control; KO, LAIFKO. All animals were 8 weeks of age unless otherwise indicated. Controls are $AIF^{flox/y}$.

secretion (Figure 8D). These indications of improved insulin sensitivity in Hq mice were confirmed using an insulin tolerance test (Figure S8A). Importantly, Hq mice also displayed virtually complete resistance to diet-induced diabetes (Figure 8D; Figure S8B). We confirmed these data at several ages up to 8 months (data not shown), a time point after which the neurodegenerative effects of global OxPhos defects begin to surface in the Hq mouse (van Empel et al., 2005). Thus, the generalized OxPhos deficit in the Hq mouse does not predispose toward insulin resistance and results in a diabetes- and obesity-resistant metabolic phenotype.

Improved Glucose Tolerance of AIF-Deficient Mice Is Both Inducible and Reversible

To address the causality of AIF modulations on mitochondrial function and glucose tolerance, we designed two adenoviral transgene delivery protocols to induce and rescue the observed phenotypes. First, we performed AIF gene ablation in 7 week old adult $AIF^{flox/flox}$ mice using adenoviral delivery of Cre recombinase. As reported previously for other floxed alleles (Lee et al., 1997) adenovirus-Cre resulted in predominant deletion of AIF in the liver (Figure S8C). Within 2 weeks we observed marked downregulation of AIF protein expression (Figure 8E) and impaired mitochondrial function as determined by reduced complex I activity (Figure 8F). Importantly, when challenged with glucose, mice with such acute deletions of AIF exhibited both markedly reduced peak blood glucose (Figure 8G) and decreased plasma insulin levels (Figure 8H).

We next performed an in vivo rescue experiment to test the reversibility of the AIF phenotype. A cohort of LAIFKO mice was injected with adenoviruses carrying a wild-type AIF transgene. In vivo delivery of AIF indeed increased AIF protein levels in the liver of LAIFKO mice (Figure 8I).

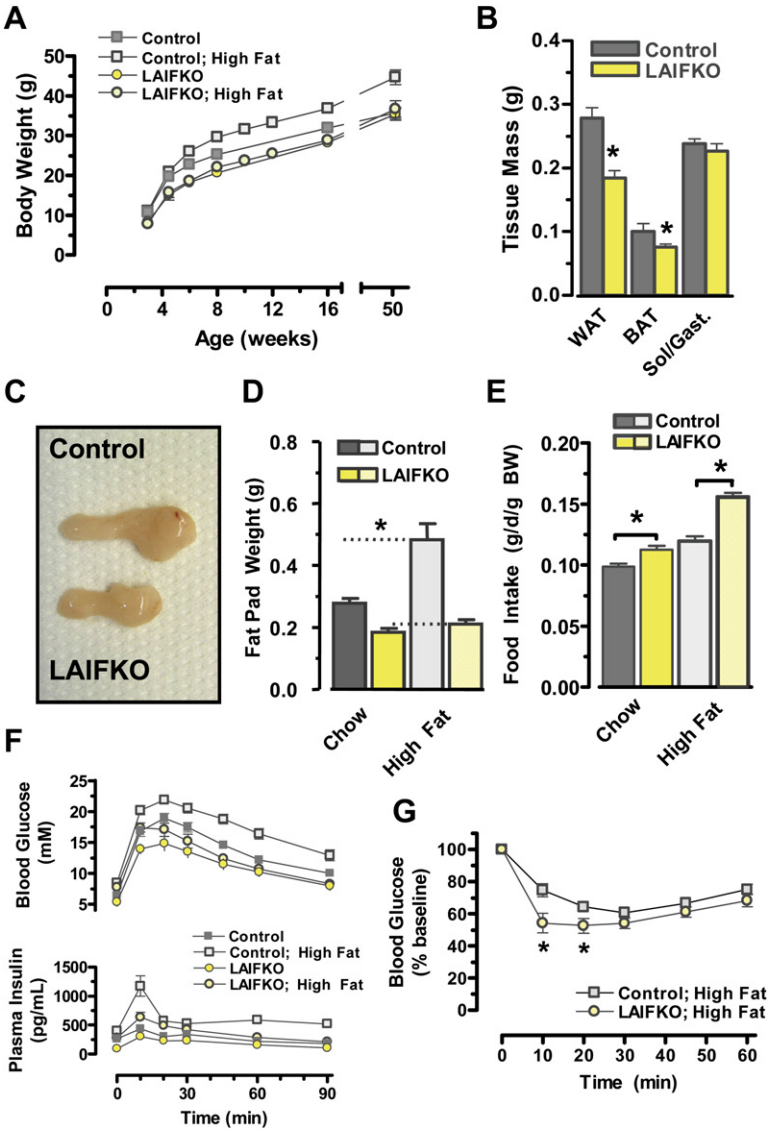

Figure 7. Liver-Specific AIF Knockout Mice Are Resistant to Obesity and Diabetes

(A) LAIFKO mice are spared from the weight gain associated with chronic high-fat feeding.

(B–D) Fat deposition is reduced in 8-week-old LAIFKO mice both after normal chow feeding and after 5 weeks of a high-fat diet. Sol/Gast., soleus and gastrocnemius; WAT, white (perigonadal) adipose tissue; BAT, brown adipose tissue.

(E) The observed reductions in adiposity of LAIFKO mice occur despite significant increases in food intake. Food intake was measured over 48 hr in metabolic cages.

(F) A 1 g/kg OGTT revealed that LAIFKO mice resist the diabetogenic effects associated with a hypercaloric feeding. OGTTs were performed on 8-week-old mice, after 5 weeks of high-fat feeding.

(G) High-fat fed LAIFKO mice maintain an increase in insulin sensitivity following an i.p. insulin challenge (1.5 U/kg). Data are mean ± SEM. n = 6–10 animals per group. *p < 0.05 versus control. All mice were 8 weeks of age. Controls are *AIF*$^{flox/y}$.

Remarkably, expression of transgenic AIF elicited a robust rescue of glucose tolerance (Figure 8J). In addition, plasma peak insulin levels were restored to near normal in LAIFKO mice 1 week after delivery of the wild-type AIF transgene (Figure 8K). These data show that acute changes in AIF expression can both induce and reverse mitochondrial dysfunction and, most importantly, improve glucose tolerance in mice.

DISCUSSION

To test the hypothesis that reduced OxPhos causes insulin resistance, we needed to develop a genetic model system that closely mimicked previously reported OxPhos defects in prediabetic humans. We therefore generated and tested the applicability of muscle- and liver- specific AIF knockout mice. Three criteria were used: the model should demonstrate a (1) mild, (2) generalized, and (3) ROS-dissociable OxPhos deficit. Using protein and RNA analyses coupled with functional biochemistry in mitochondria, we established that MAIFKO and LAIFKO mice display subtle reductions in expression of OxPhos genes from all respiratory chain complexes. These changes were manifest functionally in both muscle- and liver-specific knockouts and overlap >90% with the human data sets first identifying coordinate downregulation of OxPhos genes as a potential cause of insulin resistance (Mootha et al., 2003; Patti et al., 2003). In addition to a coordinate reduction in OxPhos gene expression, examination of isolated AIF-deficient mitochondria revealed a tightening of respiratory control and shifted substrate selectivity culminating in an OxPhos deficiency dissociable from ROS accumulation, suggesting a novel role for AIF in the control of electron flow through the respiratory chain. Thus, using *AIF*-conditional mutant mice, we asked whether a primary OxPhos defect triggers insulin resistance and diabetes

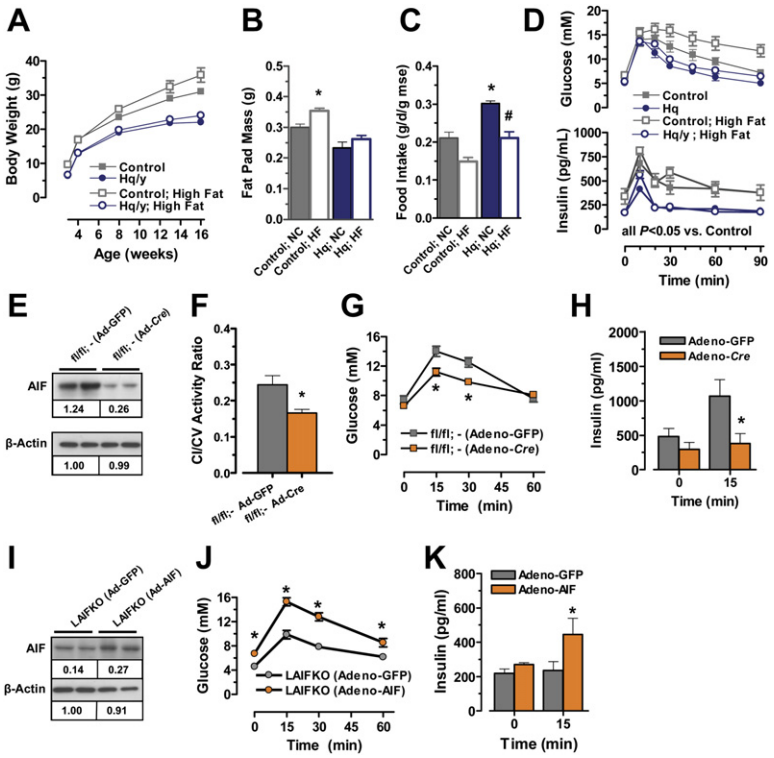

Figure 8. Insulin-Sensitive States Resulting from AIF Deletion Are Inducible, Reversible, and Maintained under Ubiquitous Hypomorph Conditions

Relative to littermate controls (gray squares), the ubiquitous *Aif*-hypomorph, the *harlequin* mouse (blue circles), demonstrates a nearly identical metabolic phenotype to MAIFKO and LAIFKO mice with reduced (A) body weight and (B) perigonadal adipose deposition in response to high-fat feeding (open symbols) despite (C) hyperphagia. (D) *Harlequin* mice exhibit greatly improved glucose tolerance in response to a 1 g/kg oral glucose load. (E–K) Seven-week-old $AIF^{flox/flox}$ mice were administered 2 × 10^9 pfu of either Adeno-*Cre* or Adeno-GFP in PBS via the tail vein. (E) Robust decreases of AIF protein level were detectable in Adeno-*Cre*-induced liver relative to controls (Adeno-GFP). (F) Liver samples obtained from *Cre*-induced animals exhibited significant decreases in Complex I activity. (G and H) Oral glucose tolerance (1 g/kg) showed significant improvement in both (G) glucose and (H) insulin levels consistent with increased insulin sensitivity. (I) Parallel i.v. administration of Adeno-AIF into LAIFKO mice significantly raised AIF protein levels in the liver compared to Adeno-GFP treated LAIFKO littermate controls. (J) Within 1 week after transgene delivery the Adeno-AIF group displayed significantly elevated fasting and peak blood glucose levels during an OGTT and (K), similarly, increases in peak plasma insulin. Data are mean ± SEM. n = 6–10 animals per group. *$p < 0.05$ versus control normal chow, #$p < 0.05$ versus high-fat diet fed controls. NC, normal chow diet; HF, high fat diet. All mice were 8 weeks of age.

and, importantly, dissociates these phenotypes from the interference of ROS accumulation.

We have previously reported cardiomyopathy and muscle wasting at late stages in the muscle-specific *AIF* knockouts (Joza et al., 2005; Wang et al., 2001; Wang et al., 1999). To rule out potential interference of such alternate pathologies in MAIFKO mice, numerous measures were undertaken. First, backcrossing the conditional AIF mouse onto the C57BL/6 background slowed the manifestation of the OxPhos defect and associated myopathies significantly; 8-week-old MAIFKO mice showed no measurable morphological, histological, serum, or intracellular signaling signs of muscle wasting, cardiomyopathy, or associated cachexia. MAIFKO showed normal heart-weight ratios at 8 weeks of age, displayed normal glucose uptake in the heart in vivo, and contrary to predictions for a (pre-)cachectic state, food intake was increased. We also exploited *AIF*'s presence on the X chromosome to generate a set of mice with a mosaic muscle-specific *AIF* knockout pattern based upon random epigenetic X-inactivation ($AIF^{flox/+}$; Mck-cre/+). These mice live long, full lives with no signs of muscle wasting or cardiomyopathy. As a final genetic control to exclude alternate pathologies, we performed AIF gene ablation in 7-week-old adult $AIF^{flox/flox}$ mice using adenoviral delivery of Cre recombinase and an in vivo rescue experiment to test the reversibility of the AIF phenotype. Acute changes in AIF expression could indeed induce and reverse mitochondrial dysfunction and, most importantly, improve glucose tolerance in adult mice in vivo.

To date, a number of studies have linked reduced mitochondrial oxidative metabolism to the development of insulin resistance in humans (Lowell and Shulman, 2005; Wisløff et al., 2005; Rabol et al., 2006; Mootha et al., 2003; Patti et al., 2003), though none have demonstrated a causal link. In addition, a recent study using a pharmacological approach suggested that improving mitochondrial function protects from diabetes and obesity (Lagouge et al., 2006). Mechanistically, it is proposed that insulin resistance caused by reduced OxPhos results from the accumulation of metabolites such as ROS and long chain fatty acids which then cause insulin resistance (Lowell and Shulman, 2005). Although we cannot exclude that specific patterns of OxPhos dysfunction may be causative for insulin resistance, our data show that a mild and generalized OxPhos deficit absent of ROS generation can culminate in a state of reduced adiposity and increased insulin sensitivity, an important contradiction of the current dogma. Similar to human studies correlating OxPhos and insulin resistance across a range of ages (Petersen et al., 2003, 2004) our data in young and old mice indicate that the beneficial effects of defective OxPhos appear to be independent of age. Support for our findings was recently provided by a study showing that mice carrying a muscle-specific deletion of the mitochondrial

transcription factor Tfam do not develop insulin resistance (Wredenberg et al., 2006). Tfam controls expression of all mitochondrial encoded genes including those coding for numerous OxPhos subunits, and its deletion is well accepted to cause marked respiratory deficiency. While the previously reported effects of *tfam* deletion such as ROS generation, muscle atrophy, or body weight were not examined, this study supports the data presented here, questioning a causal role for OxPhos reductions in the development of insulin resistance (Wang et al., 1999, 2001; Wredenberg et al., 2006).

How might such an OxPhos-dependent compensatory mechanism work? The OxPhos reductions observed in MAIFKO and LAIFKO mice produce three primary metabolite shifts (decreased ATP, decreased NAD^+, and increased AMP) and promote anaerobic glucose metabolism. To compensate for the relative inefficiency of anaerobic metabolism and aerobic substrate shifts, a net increase in fuel utilization (glucose and fatty acid metabolism) is required to meet energy demands. This inefficient utilization of fuels likely accounts for the failure of our OxPhos-deficient mice to increase their fat body mass even in the context of increased caloric intake. Furthermore, activation of AMPKinase stimulates catabolic processes such as glucose uptake and fatty-acid oxidation (Towler and Hardie, 2007). Finally, reduced NAD^+ levels, observed in both MAIFKO and LAIFKO mice, have been shown to reduce activation of the SIRT1/PGC1α pathway promoting glycolysis and, thus, exacerbating the anaerobic phenotype (Rodgers et al., 2005). These effects coincide precisely with the observed metabolic changes in *AIF* deficient mice, namely increased glucose utilization, increased glycolysis, and reduced lipid storage. Thus, our data imply that a primary OxPhos defect results in increased glucose uptake and enhanced fuel utilization.

Recent studies have placed altered mitochondrial oxidative phosphorylation in muscle and liver as an underlying genetic element of insulin resistance (Lowell and Shulman, 2005; Misu et al., 2007; Mootha et al., 2003; Patti et al., 2003; Petersen et al., 2003, 2004; Rabol et al., 2006). However, the causative or compensatory nature of these OxPhos changes has never been experimentally proven. Our data in four different mouse models of tissue specific and global OxPhos deficiency show that a primary OxPhos defect alone does not cause diabetes but, rather, can result in increased insulin sensitivity and resistance to diabetes and obesity. Importantly, acute induction and rescue experiments indicate a causal link between AIF-modulation and insulin sensitivity, absent of secondary body weight compensations. These findings carry profound implications for basic physiology and the development of future antidiabetic therapies.

EXPERIMENTAL PROCEDURES

Generation of Tissue-Specific AIF Knockout Mice

Mice with a conditional *Aif* allele were generated by homologous recombination (Joza et al., 2005). Aif^{flox} mice were backcrossed >8 times onto the C57/Bl6 background prior to initiation of the current studies. Mice with a targeted deletion of AIF in striated muscle were generated by crossing the $Aif^{flox/+}$ mice with transgenic mice expressing *Cre*-recombinase under the control of the muscle creatine kinase promoter (Mck-*cre*) (Bruning et al., 1998). $Aif^{flox/+}$ female mice bearing the *cre*-transgene established a second model, one of mosaic AIF deletion in striated muscle due to random expression of either the floxed or WT allele in any single myocyte. Crossing the conditional line to mice expressing *Cre*-recombinase under control of the Albumin promoter yielded the third model, liver-specific AIF knockout mice. Harlequin mice were obtained from Jackson Laboratories (USA). Normal chow (6% fat; M-Z, energy rich) and high-fat (30% fat; EF1/22) diets were obtained from Ssniff GmbH, Germany. Mice were fed the high-fat diet starting from 3 weeks of age until termination of the experiments. Animals were kept on a 12 hr light/dark cycle and housed at the IMBA Animal Facility in accordance with institutional guidelines.

Assessment of Mitochondrial Function

For the isolation of mitochondria, hindlimb muscle, or total liver from MAIFKO or LAIFKO mutant mice and their respective and littermate controls were homogenized (250 mM sucrose, 5 mMTris-HCl, 2 mM EGTA [pH 7.2]) at 4°C. Homogenate was centrifuged at 760 × g for 10 min at 4°C to remove nuclei and cellular debris. The supernatant was then centrifuged at 8,740 × g. The pellet was resuspended, layered onto a 60%–30%–18% sucrose Percoll gradient, and centrifuged at 8,460 × g. Activities of complexes I to IV were spectrophotometrically measured using a dual-wavelength spectrophotometer (SLM-Aminco DW-2A; SLM Instruments, Inc., Urbana, IL) (Chretien et al., 1994). Measurements of NADH oxidation were performed by polarography (Benit et al., 2006).

Glucose and Insulin Tolerance Tests

Following an overnight fast, mice were administered glucose (1 g/kg) by oral gavage, and blood samples for glucose and insulin determination were collected from the tail vein at the indicated times. Insulin tolerance was assessed after a 2 hr fast by administration of human insulin (0.75 U/kg i.p.; 1.5 U/kg after high-fat feeding) and blood glucose monitoring. Glycemia was assessed using a SureStep Ultra (Lifescan) glucometer. Insulin determinations were made using a low sample volume insulin ELISA (Crystal Chemistry).

Hyperinsulinemic Clamps and Whole-Body Glucose Turnover

Hyperinsulinemic clamps were performed as described (Knauf et al., 2005). In brief, an indwelling catheter was placed into the left femoral vein and externalised in the interscapular region. The animals were allowed to recover for 5 days and fasted for 6 hr on the day of the experiment. For 3 hr D-[3-^{3}H]-glucose was infused at a rate of 30 μCi/kg/min and insulin at a rate of either 4 mU/kg/min (LAIFKO) or 18 mU/kg/min (MAIFKO and LAIFKO). Low insulin infusions were used to assess hepatic insulin sensitivity while high insulin was used to assess muscle insulin sensitivity. Euglycemia was maintained by variable infusion of 15% glucose. Whole blood was sampled from the tail every 10 min during the last hour. Total radioactivity in the supernatant was determined by scintillation counting. Total glucose concentrations were determined by the glucose oxidase method (BioMerieux). Glycogen content was determined in quadriceps muscle and liver using the amyloglucosidase method. Released glucose was determined by a glucose oxidase method (BioMerieux). Plasma T3, T4, and cortisol levels, as well as the muscle and liver enzyme panels, were determined by an analytical laboratory (InVitro, Austria), while the inflammatory markers TNF-α, IL-6, resistin, as well as leptin, were determined using a multiplex kit from Linco Research (USA).

Indirect Calorimetry

Mice were placed for 48 hr in metabolic cages connected to an open-circuit, indirect calorimetry system combined with the determination of

spontaneous activity by beam breaking (Oxylet, Panlab-Bioseb, Chaville France). The animals were accustomed to the apparatus during the first 24 hr, followed by measurement for a further 24 hr. Oxygen consumption and carbon dioxide production were recorded at 5 min intervals using a computer-assisted data acquisition program (Chart 5.2, AD Instruments, Sydney, Australia).

Tissue Glucose Utilization

Mice were injected with ^{3}H-2 deoxyglucose (Perkin Elmer) through the intrafemoral catheter one hour before completion of the infusion procedure (Knauf et al., 2005). Tail blood was sampled at 5, 10, 15, 20, 30, 45, and 60 min after the injection to determine the time course of ^{3}H-2 deoxyglucose disappearance. The ^{3}H-2 deoxyglucose-6-phosphate content was determined from NaOH hydrolysed tissues by the Somogyi procedure (Somogyi, 1945).

Western Blotting

Tissue samples were snap frozen, pulverized, and dispersed in lysis buffer (0.02 M Tris, 1% NP40, 0.15 M NaCl, 0.15 M NaF, 2 mM Na_3VO_4, 5 mM EDTA, + Complete cocktail protease inhibitors). 40 μg of sample were loaded onto 4%–12% gradient gels (Invitrogen) and blotted. All antibodies were obtained from Cell Signaling except antibodies for respiratory chain subunits (Molecular Probes), CD36 and AIF (Chemicon), GLUT1 and GLUT4 (Abcam).

Microarray Analyses

Three independent microarray analyses were performed using hindlimb and total RNA preparations from BMI-matched MAIFKO and LAIFKO mice and their respective *AIF*$^{flox/y}$ littermates. Briefly, after linear amplification and reverse transcription in the presence of Cy3-dUTP or Cy5-dUTP, cDNA probes were ethanol precipitated together with poly-dA, tRNA, and mouse Cot.1 DNA. Following posthybridization washing (0.2× SSC, 0.1% SDS), the slides were dried and scanned (Axon GenePix 4000). Results were normalized using the Bioconductor marray package, and the "Print Tip Loess" Algorithm. The cDNA microarrays were compiled and printed from 26,000 EST clones (BMAP and NIA clones) corresponding to 17,000 Unigene clusters. Gene ontology-based scoring was performed using pathway sets curated from the Biocarta and KEGG databases (www.biocarta.com and http://www.genome.jp/kegg/pathway.html) (Tomfohr et al., 2005).

Determination of Intracellular Metabolites

Measurements of NAD/NADH, ATP, cAMP, catalase, and protein carbonylation were determined in freshly isolated hindlimb muscle or liver from 4, 8, and 16 week old male MAIFKO, LAIFKO, and their respective controls. NAD/NADH levels were determined by an enzyme cycling method in acid or base extracted sample (Lin et al., 2001). ATP and cAMP levels were assessed using commercially available assays (ATP CLS II, Roche; cAMP [low pH] immunoassay, R&D Systems). ROS generation was measured directly by EPR-spectroscopy on isolated mitochondria and indirectly using kits for catalase activity, protein carbonylation, and lipid peroxidation (Cayman Chemicals and Oxis International, USA). In brief, EPR-spectroscopic detection of ROS generation was performed by mixing isolated mitochondria with 20 μM of either of the spin trap compounds, CPH (1-hydroxy-3-carboxy-pyrrolidine) or PPH (1-hydroxy-4-phosphonooxy-2,2,6,6-tetramethylpiperidine). EPR measurements were performed on a Bruker EMX EPR spectrometer (BioSpin GmbH Rheinstetten/Karlsruhe, Germany).

Histology and Mitochondrial DNA Quantification

Unless otherwise indicated, all tissue samples were obtained from 8-week-old male littermates. Samples for light microscopy were fixed in 4% PFA for 1 hr. Paraffin embedding, sectioning, and H&E staining were performed according to standard protocols. Transmission electron microscopy was performed after a 1 hr fixation in 2% Gluteraldehyde/1% PFA in Cacodylate buffer (pH 7.4), and postfixation treatments with 1% OsO_4 and 1% uranyl acetate. MtDNA content of muscle was determined by realtime PCR using primers specific for the murine mitochondrial encoded proteins ND1 (forward: AGGGTAC ATACAACTACGAAAAGGCC, reverse: GAGTATTTGGAGTTTGAGGC TCATCC) and COX (forward: TTGGAGGCTTTGGAAACTGACTTG, reverse: CAGTACGGCTGTAATAAGTACGGATCAG). Values were related to tubulin as a nuclear DNA control.

Adenoviral Delivery

Adeno-AIF was a kind present from Dr. R. Slack, Ottawa (Canada). Adeno-*Cre* and Adeno-GFP were obtained commercially from Vector Biolabs (USA). All three adenoviral constructs were driven by the CMV promoter and coded additionally for GFP. Viruses were diluted to a concentration of 1×10^{9} pfu/5 g body weight in 200 μl of PBS and injected into the tail vein of recipient mice.

Statistical Analysis

All data are shown as mean ± SEM. Measurements at single time points were analyzed by ANOVA or if appropriate by t test. Time courses were analyzed by repeated-measurements (mixed model) ANOVA with Bonferroni post-tests. All statistical tests were calculated using the GraphPad Prism 4.00 (GraphPad Software, San Diego, CA, USA). $p < 0.05$ was considered to indicate statistical significance.

Supplemental Data

Supplemental Data include eight figures and four tables and can be found with this article online at http://www.cell.com/cgi/content/full/131/3/476/DC1/.

ACKNOWLEDGMENTS

The authors would like to thank J.A. Ehses, M. Roden, G. Obernosterer, and S. O'Rahilly for critical discussion. Also we are endebted to G. Resch, M. Brandstetter, M. Rangachari, P. Steinlein, V. Komenovic, M. Radolf, L. Montbrun, L. Klein, T. Behling, S. Haindl, L. Pénicaud, and the Toulouse Genopole for technical help. J.A.P., G.N., and T.N. are funded by IIF fellowships of the Marie Curie Foundation, P.D.C. from the FNRS, Belgium. C.R.K. is supported by NIH grant DK31036. J.M.P. is supported by IMBA, the Austrian Ministry of Science and Education, and the Austrian National Bank. R.B. is the recipient of grants for the ATIP-CNRS program as well as the "Programme national de recherche en alimentation et nutrition humaine 2005 nos. 5–13." I.E. greatly appreciates financial support by the Wiener Wissenschafts-, Forschungs- und Technologiefonds (WWTF). P.B. and P.R. were supported by the Integrated European Project Eumitocombat and the Association Française contre les Myopathies.

Received: April 6, 2007
Revised: July 2, 2007
Accepted: August 29, 2007
Published: November 1, 2007

REFERENCES

Adam-Vizi, V., and Chinopoulos, C. (2006). Bioenergetics and the formation of mitochondrial reactive oxygen species. Trends Pharmacol. Sci. *27*, 639–645.

Balaban, R.S., Nemoto, S., and Finkel, T. (2005). Mitochondria, oxidants, and aging. Cell *120*, 483–495.

Benit, P., Goncalves, S., Philippe Dassa, E., Briere, J.J., Martin, G., and Rustin, P. (2006). Three spectrophotometric assays for the measurement of the five respiratory chain complexes in minuscule biological samples. Clin. Chim. Acta *374*, 81–86.

Boushel, R., Gnaiger, E., Schjerling, P., Skovbro, M., Kraunsoe, R., and Dela, F. (2007). Patients with type 2 diabetes have normal mitochondrial function in skeletal muscle. Diabetologia *50*, 790–796.

Bruning, J.C., Michael, M.D., Winnay, J.N., Hayashi, T., Horsch, D., Accili, D., Goodyear, L.J., and Kahn, C.R. (1998). A muscle-specific insulin receptor knockout exhibits features of the metabolic syndrome of NIDDM without altering glucose tolerance. Mol. Cell *2*, 559–569.

Cheung, E.C., Joza, N., Steenaart, N.A., McClellan, K.A., Neuspiel, M., McNamara, S., MacLaurin, J.G., Rippstein, P., Park, D.S., Shore, G.C., et al. (2006). Dissociating the dual roles of apoptosis-inducing factor in maintaining mitochondrial structure and apoptosis. EMBO J. *25*, 4061–4073.

Chretien, D., Rustin, P., Bourgeron, T., Rotig, A., Saudubray, J.M., and Munnich, A. (1994). Reference charts for respiratory chain activities in human tissues. Clin. Chim. Acta *228*, 53–70.

Dahlman, I., Forsgren, M., Sjogren, A., Nordstrom, E.A., Kaaman, M., Naslund, E., Attersand, A., and Arner, P. (2006). Downregulation of Electron Transport Chain Genes in Visceral Adipose Tissue in Type 2 Diabetes Independent of Obesity and Possibly Involving Tumor Necrosis Factor-{alpha}. Diabetes *55*, 1792–1799.

Houstis, N., Rosen, E.D., and Lander, E.S. (2006). Reactive oxygen species have a causal role in multiple forms of insulin resistance. Nature *440*, 944–948.

Joza, N., Oudit, G.Y., Brown, D., Benit, P., Kassiri, Z., Vahsen, N., Benoit, L., Patel, M.M., Nowikovsky, K., Vassault, A., et al. (2005). Muscle-specific loss of apoptosis-inducing factor leads to mitochondrial dysfunction, skeletal muscle atrophy, and dilated cardiomyopathy. Mol. Cell. Biol. *25*, 10261–10272.

Knauf, C., Cani, P.D., Perrin, C., Iglesias, M.A., Maury, J.F., Bernard, E., Benhamed, F., Gremeaux, T., Drucker, D.J., Kahn, C.R., et al. (2005). Brain glucagon-like peptide-1 increases insulin secretion and muscle insulin resistance to favor hepatic glycogen storage. J. Clin. Invest. *115*, 3554–3563.

Lagouge, M., Argmann, C., Gerhart-Hines, Z., Meziane, H., Lerin, C., Daussin, F., Messadeq, N., Milne, J., Lambert, P., Elliott, P., et al. (2006). Resveratrol improves mitochondrial function and protects against metabolic disease by activating SIRT1 and PGC-1alpha. Cell *127*, 1109–1122.

Lane, N. (2006). Mitochondrial disease: Powerhouse of disease. Nature *440*, 600–602.

Lazar, M.A. (2005). How obesity causes diabetes: Not a tall tale. Science *307*, 373–375.

Lee, Y.H., Sauer, B., Johnson, P.F., and Gonzalez, F.J. (1997). Disruption of the c/ebp alpha gene in adult mouse liver. Mol. Cell. Biol. *17*, 6014–6022.

Lin, S.S., Manchester, J.K., and Gordon, J.I. (2001). Enhanced gluconeogenesis and increased energy storage as hallmarks of aging in Saccharomyces cerevisiae. J. Biol. Chem. *276*, 36000–36007.

Lowell, B.B., and Shulman, G.I. (2005). Mitochondrial dysfunction and type 2 diabetes. Science *307*, 384–387.

Misu, H., Takamura, T., Matsuzawa, N., Shimizu, A., Ota, T., Sakurai, M., Ando, H., Arai, K., Yamashita, T., Honda, M., and Kaneko, S. (2007). Genes involved in oxidative phosphorylation are coordinately upregulated with fasting hyperglycaemia in livers of patients with type 2 diabetes. Diabetologia *50*, 268–277.

Mootha, V.K., Lindgren, C.M., Eriksson, K.F., Subramanian, A., Sihag, S., Lehar, J., Puigserver, P., Carlsson, E., Ridderstrale, M., Laurila, E., et al. (2003). PGC-1alpha-responsive genes involved in oxidative phosphorylation are coordinately downregulated in human diabetes. Nat. Genet. *34*, 267–273.

Nakano, H., Nakajima, A., Sakon-Komazawa, S., Piao, J.H., Xue, X., and Okumura, K. (2006). Reactive oxygen species mediate crosstalk between NF-kappaB and JNK. Cell Death Differ. *13*, 730–737.

Patti, M.E., Butte, A.J., Crunkhorn, S., Cusi, K., Berria, R., Kashyap, S., Miyazaki, Y., Kohane, I., Costello, M., Saccone, R., et al. (2003). Coordinated reduction of genes of oxidative metabolism in humans with insulin resistance and diabetes: Potential role of PGC1 and NRF1. Proc. Natl. Acad. Sci. USA *100*, 8466–8471.

Petersen, K.F., Befroy, D., Dufour, S., Dziura, J., Ariyan, C., Rothman, D.L., DiPietro, L., Cline, G.W., and Shulman, G.I. (2003). Mitochondrial dysfunction in the elderly: Possible role in insulin resistance. Science *300*, 1140–1142.

Petersen, K.F., Dufour, S., Befroy, D., Garcia, R., and Shulman, G.I. (2004). Impaired mitochondrial activity in the insulin-resistant offspring of patients with type 2 diabetes. N. Engl. J. Med. *350*, 664–671.

Postic, C., Shiota, M., Niswender, K.D., Jetton, T.L., Chen, Y., Moates, J.M., Shelton, K.D., Lindner, J., Cherrington, A.D., and Magnuson, M.A. (1999). Dual roles for glucokinase in glucose homeostasis as determined by liver and pancreatic beta cell-specific gene knock-outs using Cre recombinase. J. Biol. Chem. *274*, 305–315.

Rabol, R., Boushel, R., and Dela, F. (2006). Mitochondrial oxidative function and type 2 diabetes. Appl. Physiol. Nutr. Metab. *31*, 675–683.

Rodgers, J.T., Lerin, C., Haas, W., Gygi, S.P., Spiegelman, B.M., and Puigserver, P. (2005). Nutrient control of glucose homeostasis through a complex of PGC-1alpha and SIRT1. Nature *434*, 113–118.

Somogyi, M. (1945). Determination of Blood Sugar. J. Biol. Chem. *160*, 69–73.

St-Pierre, J., Drori, S., Uldry, M., Silvaggi, J.M., Rhee, J., Jager, S., Handschin, C., Zheng, K., Lin, J., Yang, W., et al. (2006). Suppression of reactive oxygen species and neurodegeneration by the PGC-1 transcriptional coactivators. Cell *127*, 397–408.

Susin, S.A., Lorenzo, H.K., Zamzami, N., Marzo, I., Snow, B.E., Brothers, G.M., Mangion, J., Jacotot, E., Costantini, P., Loeffler, M., et al. (1999). Molecular characterization of mitochondrial apoptosis-inducing factor. Nature *397*, 441–446.

Taniguchi, C.M., Emanuelli, B., and Kahn, C.R. (2006). Critical nodes in signalling pathways: Insights into insulin action. Nat. Rev. Mol. Cell Biol. *7*, 85–96.

Tomfohr, J., Lu, J., and Kepler, T.B. (2005). Pathway level analysis of gene expression using singular value decomposition. BMC Bioinformatics *6*, 225.

Towler, M.C., and Hardie, D.G. (2007). AMP-activated protein kinase in metabolic control and insulin signaling. Circ. Res. *100*, 328–341.

Vahsen, N., Cande, C., Briere, J.J., Benit, P., Joza, N., Larochette, N., Mastroberardino, P.G., Pequignot, M.O., Casares, N., Lazar, V., et al. (2004). AIF deficiency compromises oxidative phosphorylation. EMBO J. *23*, 4679–4689.

van Empel, V.P., Bertrand, A.T., van der Nagel, R., Kostin, S., Doevendans, P.A., Crijns, H.J., de Wit, E., Sluiter, W., Ackerman, S.L., and De Windt, L.J. (2005). Downregulation of apoptosis-inducing factor in harlequin mutant mice sensitizes the myocardium to oxidative stress-related cell death and pressure overload-induced decompensation. Circ. Res. *96*, e92–e101.

Wallace, D.C. (1999). Mitochondrial diseases in man and mouse. Science *283*, 1482–1488.

Wang, J., Silva, J.P., Gustafsson, C.M., Rustin, P., and Larsson, N.G. (2001). Increased in vivo apoptosis in cells lacking mitochondrial DNA gene expression. Proc. Natl. Acad. Sci. USA *98*, 4038–4043.

Wang, J., Wilhelmsson, H., Graff, C., Li, H., Oldfors, A., Rustin, P., Bruning, J.C., Kahn, C.R., Clayton, D.A., Barsh, G.S., et al. (1999). Dilated cardiomyopathy and atrioventricular conduction blocks induced by heart-specific inactivation of mitochondrial DNA gene expression. Nat. Genet. *21*, 133–137.

Wisløff, U., Najjar, S.M., Ellingsen, O., Haram, P.M., Swoap, S., Al-Share, Q., Fernström, M., Rezaei, K., Lee, S.J., Koch, L.G., and Britton, S.L. (2005). Cardiovascular risk factors emerge after artificial selection for low aerobic capacity. Science *307*, 418–420.

Wissing, S., Ludovico, P., Herker, E., Buttner, S., Engelhardt, S.M., Decker, T., Link, A., Proksch, A., Rodrigues, F., Corte-Real, M., et al. (2004). An AIF orthologue regulates apoptosis in yeast. J. Cell Biol. *166*, 969–974.

Wredenberg, A., Freyer, C., Sandstrom, M.E., Katz, A., Wibom, R., Westerblad, H., and Larsson, N.G. (2006). Respiratory chain dysfunction in skeletal muscle does not cause insulin resistance. Biochem. Biophys. Res. Commun. *350*, 202–207.

Accession Numbers

Microarray data can be found at http://www.ncbi.nlm.nih.gov/projects/geo/query/acc.cgi?acc=GSE8905, accession number GSE8905.